Indian Journal of Pure & Applied Physics
Vol. 61, January 2023, pp. 19-26
DOI: 10.56042/ijpap.v61i1.68529

Extensibility of External Magnetic Potential at High Latitudes - Antarctica

C P Anil Kumar[a*], J C K Akhila[b] & Ann Sherin A[b]

[a]Equatorial Geophysical Research Laboratory, Indian Institute of Geomagnetism, Krishnapuram, Tirunelveli, Tamil Nadu, 627 011, India

[b]School of Pure & Applied Physics, M.G. University, Kottayam, Kerala, 686 560, India

Received 12 November 2022; accepted 22 December 2022

We investigated the external magnetic potential due to solar forcing, with nine years of data during 2001-2009, covering the deep solar minimum (2006-2009), at two stations: one is in the polar cap -Vostok (78º27'S, 106º52'E; mag. lat 83°S) and another is in the subauroral region - Maitri (70º45'S, 11º43'E: mag. lat 67^{0}S) in Antarctica. The significance of the work is associated with space weather prediction and its impact on planet Earth. We used Advance Composition Explorer (ACE) satellite data for the aforesaid period for a thorough understanding of influences due to solar wind origin and to compare the parameter observed in these regions. We used the spherical cap harmonic analysis (SCHA) function as a tool. The inference indicates that at Vostok the magnitude is enhanced throughout and depicts a broad ambient external magnetic potential. It seems to be essentially the intensification of the region 1 currents whereas at Maitri intense electric fields are produced during geomagnetic perturbations which drive a system of disturbed time Region 2 currents over the quiet time currents. During this scenario in Maitri there are noticeable peaks or enhancements in the magnetic potential that can be observed mainly during geomagnetic disturbances. Hence the regression relation developed for external magnetic potential calculation, in terms of solar wind parameters agrees well with polar cap region and the area is relatively less explored earlier, the present investigation can be expected to add knowledge about that regime.

Keywords: Antarctica; External magnetic potential; Electrodynamics; Global electric circuit; Spherical cap harmonic analysis

1 Introduction

It is well known that magnetism is a fundamental property and its existence was known for centuries. In 1600 AD, William Gilbert first pointed out that the Earth itself behaved like a huge magnet. It was noted that Earth's magnetic field extended from the Earth's interior and transverses external to the Earth's surface and up to interplanetary space. The geomagnetic maps were made of geomagnetic elements. Regular and systematic investigation of geomagnetic behavior started in the eighteen century[1]. Chapman and Ferraro[2] noticed that magnetic perturbations are produced by the electric currents in the ionosphere and magnetosphere by the induced emf when the conductivity is generated due to the electric field generated in the ionosphere and magnetosphere.

We know that the points at which the geomagnetism is strongest are called the poles and the magnetic poles of Earth are not fixed, but wander over time[3]. Because of the convective motions of the molten fluid plasma above the solidified inner core, geodynamo is developed which gives rise to the Earth's magnetism. The main internal component of geomagnetism has been attributed to the contribution from the Earth's core. A minor fraction of geomagnetism is due to magnetic ore in the crust and ionospheric E-regional dynamo. As such, the observed spatial and temporal variations of the geomagnetic field have two distinct sources viz., the internal one as cited and the external one due to the solar wind dynamo, the magnetic field generated by an interplanetary of the electric field in IMF. In general, the short-period variations of the geomagnetic field have an external origin, while long-period variations are mainly due to internal origin. The current research work is an attempt to account for the variation of the magnetic potential of external origin. External magnetic potential rise when the IMF of the solar wind couples with the Earth's magnetic field lines under specific conditions. This energy transferred to the Earth system can be estimated with the aid of coupling functions, as briefed [4].

The coupling function is most widely used as it quantifies the energy transfer in terms of power and the time-integrated values can be compared to estimate energy sinks. Knipp[5], studied an event-specific origin-to-end view of the geomagnetic storm

Corresponding author: (E-mail: anilkumar.cp@iigm.res.in)

event. Lu[6] used the coupling parameter to quantify the global magnetospheric deposition during a magnetic cloud event. Stamper[7] studied the long coupling between geomagnetic activity and solar wind. Kallio[8] used Epsilon parameter[9] to study the loading-unloading processes during a substorm. Tanskanen[10] analyzed the substorm energy budget during low and high solar activities. In the last 30 years, the data and our understanding of the dissipative processes in the inner magnetosphere and ionosphere have been greatly improved and it has been generally accepted that the most important forms of energy dissipation are Joule heating of the ionosphere, ring current injection and particle precipitation. The electrodynamics and hence the magnetic potentials during this process are analyzed and discussed to gain a better understanding of how the flow of energy is transferred to the high latitude upper atmosphere when it is directed to planet Earth.

2 Materials and methods

The external component of the geomagnetic field, exhibits marked variations of both regular (recurrent) and irregular kind (non-recurrent) mainly due to solar activity[11]. It can be as small as few nT to few hundred nT in the background of a total of ten thousands of Earth's internal magnetic field. Since most of the energy is stored as potential the theory of external magnetic potential is important and theoretically proved in the following steps.

For the same, we have to consider an external magnetic field (B) or a current carrying loop, whichever may be the case the magnetic dipole experiences a torque ($\boldsymbol{\tau}$) that aligns it with the field. The torque is governed by the relationship, Eq. (1)

$$\tau = m \times B \quad \ldots (1)$$

where 'm' is the measure of its strength (magnetic moment) for a current-carrying loop, Eq. 2.

$$m = (IA)\ Am^2 \quad \ldots (2)$$

where I- current, A- area, It is normal to the plane of the loop (both m and B are assumed to be forced by current loops).

The potential 'ω' of dipole magnetic moment 'm' at a distance 'r' from its center and at an azimuth angle (θ) between the dipole axis and the radial direction can be given as $w = (\mu_0/4\pi) \times m(\cos\theta)/r^2$, where ($\mu_0 = 4\pi \times 10^{-7}$ H/m). The total dipole potential is the major component of the geomagnetic field, it represents more than 93% of its energy density and magnetic field B is the gradient of the potential $B = -\nabla W$ (w-magnetic potential). In the case of Earth, we have to consider the spherical coordinates, the field has a radial component B_r and an azimuth component B_θ (complement of the magnetic latitude).

The major part of the geomagnetic field originates from Earth's interior. Let w_i be the magnetic potential of internal origin and 'w_e' be the magnetic potential due to external origin. The total geomagnetic potential 'W' can be generally expressed as

$$W = W_i + W_e \quad \ldots (3)$$

Since Earth has spherical geometry it can be described by spherical harmonic functions of the co-latitude (θ) and longitude (Φ), as Willium[12].

$$W_e = R\Sigma_{(n=1)}^{\infty}\Sigma_{(m=0)}^{n}\left(r/R\right)^n\left(G_n^m cos(m\phi) + H_n^m sin(m\phi)\right) P_n^m cos(\theta) \quad \ldots (4)$$

for r<R, where 'R' radius of the Earth. For

$$W_i = R\Sigma_{(n=1)}^{\infty}\Sigma_{(m=0)}^{n}\left(R/r\right)^{(n-1)}\left(g_n^m cos(m\phi) + h_n^m sin(m\phi)\right) P_n^m cos(\theta) \quad \ldots (5)$$

for r>R

At Earth's surface (r/R) term vanishes and n=0, since the magnetic monopole does not exist.

It is not possible to measure the geomagnetic potential directly, so the Gauss coefficients are computed from measurements of the northward (X), eastward (Y), and vertical component (Z) above the Earth's surface.

In the north and east components, the Gauss coefficients occur as $\left(g_n^m + G_n^m\right)$ and $\left(h_n^m + H_n^m\right)$ respectively therefore the horizontal components alone do not allow separation of the external and internal parts. However, the Gauss coefficients occur in a different combination in the vertical field, and by virtue of this, the external and internal fields can be separated[13].

The magnitude of internal and external origin can be determined from the power spectrum of the Gauss coefficients. This power (energy density) associated with the coefficient of degree 'n' at the Earth's surface is given by Lowes[13], Eq.6.

$$\phi_n = (n+1)\sum\left(\left(g_n^m\right)^2\right) + \left(h_n^m\right)^2 \quad \ldots (6)$$

Geomagnetic potential decrease with radial distances as $r^{-(n+1)}$ accordingly the strength of the field varies as $r^{-(n+2)}$ since power is the square of the amplitude. This process of downward continuation of external magnetic potential due to solar disturbances is equivalent to the magnitude of external response of multi-variable function of solar wind velocity (V_{sw}), number density (N_{sw}) of solar wind (SW) IMF- B_y and B_z and clock angle (φ) of interplanetary magnetic field (IMF)[14].

So we used the advanced composition explorer satellite (ACE) data. ACE satellite provides high-resolution interplanetary magnetic field vector data (https://caltech.edu/ACE/ASC/level2). It contains a precision vector magnetometer and a cesium vapor scalar magnetometer at the end of a 6m long graphite epoxy scissors boom. The level 2 data have been used to investigate the dynamical behaviour of the geomagnetic fluctuations. The geomagnetic field data are given in Geocentric Solar Ecliptic System (GSE).

In the past, many attempts scientists have used satellite data to model the solar wind variation using Harmonic Analysis (HA)[15,16]. Other methods such as Rectangular Harmonic Analysis, Alldredge[17], Spherical Cap Harmonic Analysis, and Haines[18] have also been used. Spherical harmonic analysis has been further augmented by a physical method of regularization, Korte, and Holme[19]. Artificial Neural Networks techniques, Sutcliff [20], have also been used to model the geomagnetic daily variations and further the revised Spherical Cap Harmonic Analysis used by Weimer[14].

Magnetic potentials measurements of Maitri (70°45'S, 11°43'E: mag. lat 67°S), and Vostok (78°27'S, 106°52'E; mag. lat 83°S) were analyzed to characterize the corresponding fluctuations and plasma electrical convection pattern in subauroral latitudes and polar regions respectively using Weimer 2005-model. Since the research is the first of this kind in this region results of the previous research in the related field are not compared.

3 Results and Discussion

The most important forms of ionosphere and magnetosphere energy dissipation are Joule heating of the ionosphere, ring current injection, and particle precipitation [21,22]. In this study, other than earlier studies substorms and storms[6,23,24], the episodes of total fluctuations in Earth's horizontal magnetic field from 2001 to 2009 were studied in detail and plotted in Fig. 1 SYM-H index collected from ftp://ftp.space.dtu.dk/ WDC/indices/ used for this purpose since it is noted that the dynamical pressure changes of the solar wind are more reflected in SYM-H index than Dst index, in high latitudes[25]. Analysis of these geomagnetic parameters has many practical applications in magnetic navigation, orientation control, geophysical exploration, etc. Its difference and definitions under various geomagnetic storms have been reported[27-28]. The minimum SYM-H values are the common incident during 2008, deviations prior to the minimum value of SYM-H, normally indicate the energy-loading phase and three days after representing the energy-unloading phase. However, it is noted that this general condition varies for severe storms.

The continuous data of geomagnetic potential variation (Maitri) during solar extreme quite Julian days 220-223 in the year 2007 exhibits two types of typical external variations and it is shown in Fig. 2 (left), smooth regular variations are predominant with two peaks one at 06:00 UT and another at 20:00UT. It seems to be due to two cell convection patterns (electrical convective cells) formation[29]. Fig. 2 (right) illustrates subauroral variations during magnetic quiet days conditions during the solar active period in the year 2003. Each elementary convection cell (Fig. 3) represents a separate conductivity dynamics of the IMF interaction with the magnetosphere and its ionospheric manifestation. The activities are also due to field-aligned currents (FACs) flowing at the poleward rim of the auroral oval and ionospheric Hall currents flowing in the polar cap. These trans-polar ionospheric currents are related to the antisunward ionospheric plasma convection driven by the dawn-dusk electric fields which intern are generated by solar wind-magnetosphere interaction.

Electric fields due to the geomagnetic variations were identified at the aforesaid locations and the typical electric convective pattern is depicted in Fig. 4. During a magnetically disturbed period polar open magnetic flux extends to lower regime. Solar plasma energy is transferred at the magnetosphere dayside mainly occurring when the IMF B_Z is turned southward. Therefore more southward IMF cusp signatures can be noted than northward IMF cusp signatures. Whereas coupling occurs on the night side through the tail region which enhances the convection in the nightside ionospheric system of currents. Again intensification of currents in the auroral zone (field-aligned currents) makes magnetosphere-ionosphere coupling stronger than it's dependence on the IMF conditions.

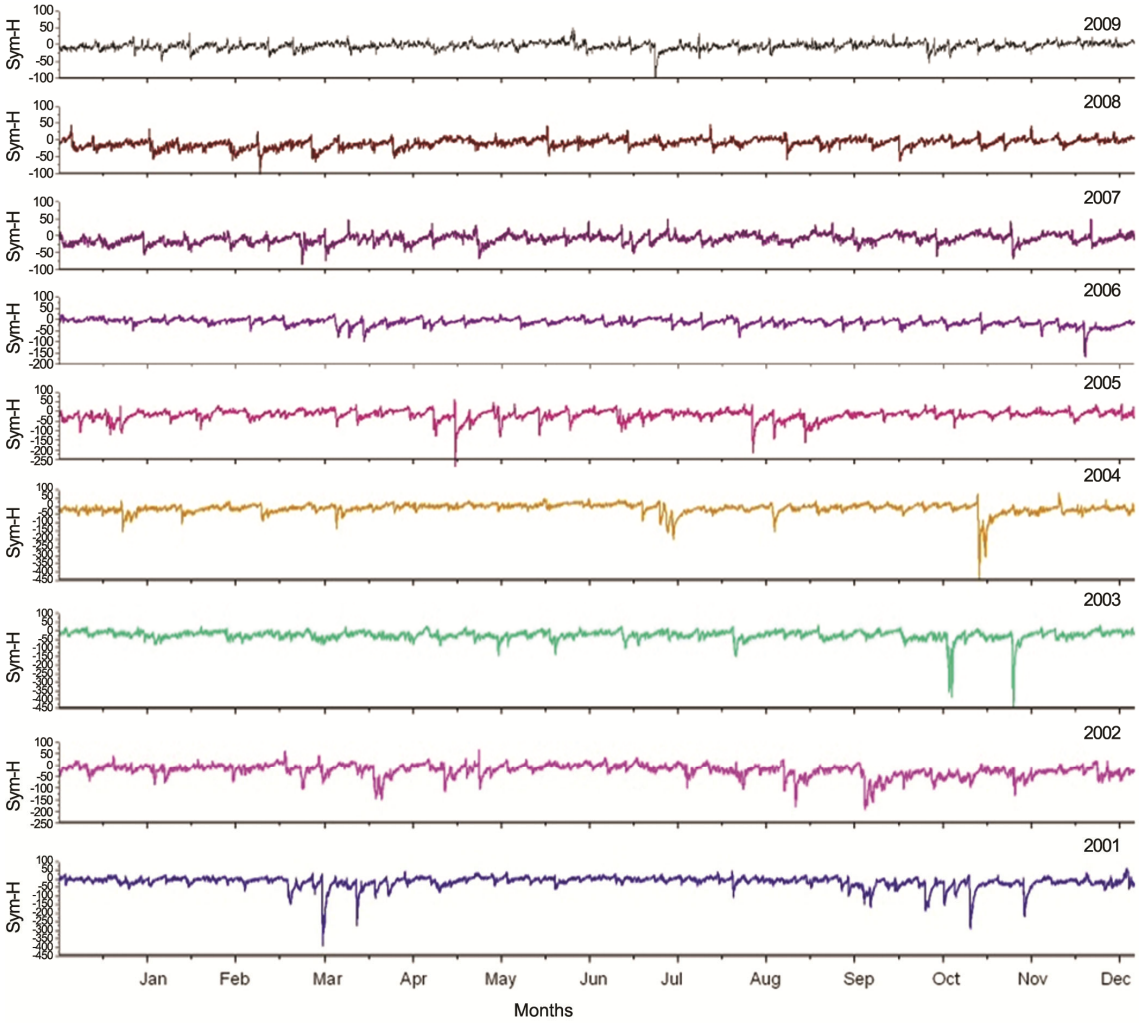

Fig. 1 — Magnetic disturbances observed in terms of Sym-H index from 2001 to 2009.

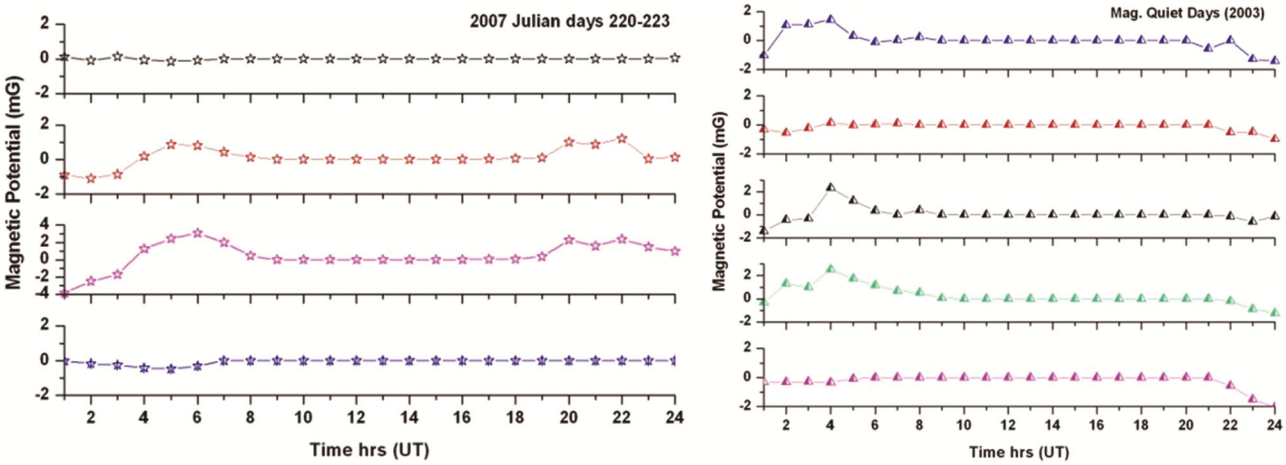

Fig. 2 — The left figure represents magnetic potential variation at sub-auroral latitude, Maitri during magnetic quite conditions during the solar minimum period Julian days 220-225 days during 2007, and the right-hand plot illustrates magnetic quite a day variations, in 2003, it was the solar maximum year.

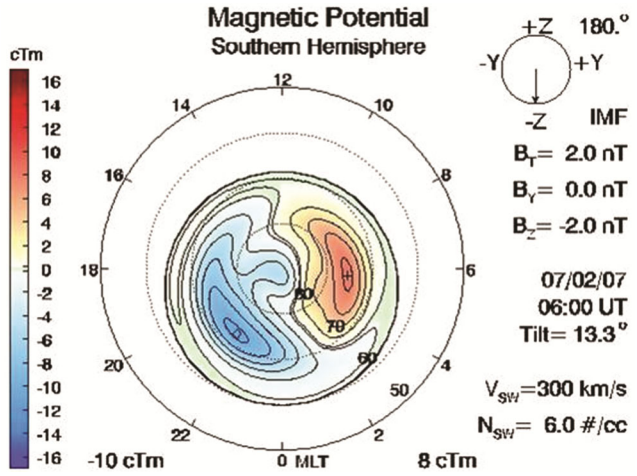

Fig. 3 — The picture indicates the dipole in southern hemisphere during a magnetic quite day. The sub-auroral latitudes showed no external magnetic perturbations.

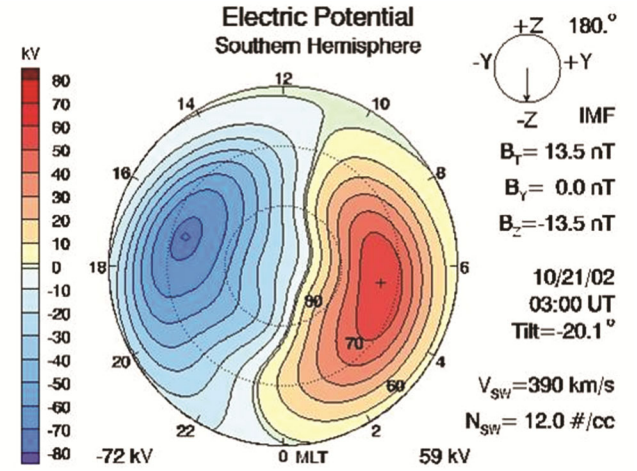

Fig. 4 — Two cell electric convection cell pattern noticed during 21 October, 2002 in the southern high latitudes generated by solar wind.

Ground based SYM-H magnetic observations at high latitudes provided the first indications that the interplanetary magnetic field was an important ordering parameter of the high latitude current system. According to Chapman and Ferraro[2], the initial magnetic disturbances caused by the magnetic cloud should resemble the field of a dipole image. To prove that we selected one such case on 21 October 2002 in the southern high latitudes, as in Fig. 4, which agrees with the above hypothesis and observations noted by Lu[6].

During magnetic disturbed days, the magnetic potential increases tenfold compared to quiet day conditions as depicted in Fig. 5. Ionospheric plasma moves along the equipotential lines viz., clockwise in the negative vortex and anti-clockwise in the positive vortex.

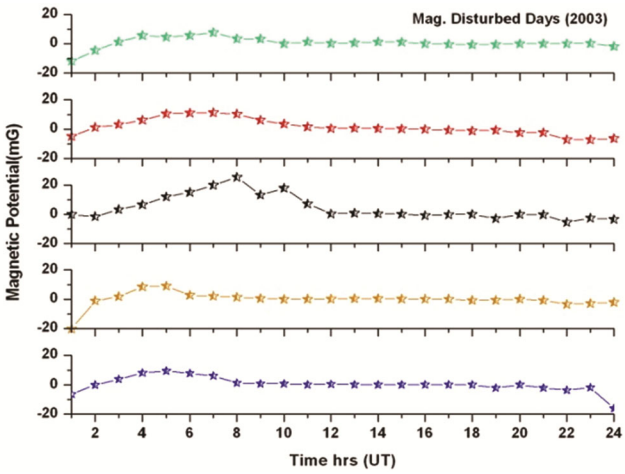

Fig. 5 — Typical magnetic potential pattern during international magnetic disturbed days of 2003.

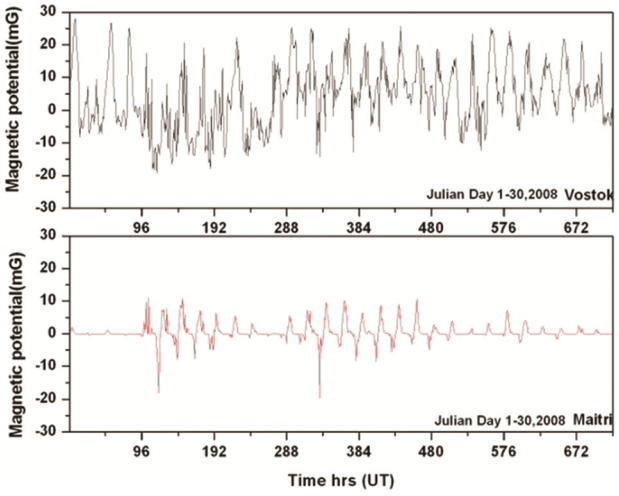

Fig. 6 — Compared the observed pattern of magnetic potential of Vostok (upper plot) and Maitri (lower plot) during the solar minimum period of 2008, Julian day 1-30.

Figure 6 compares the magnetic potential observed at Vostok and Maitri from Julian day 1 to 30, 2008. We agree with Papitashvili[30], observations that the polar region is always filled with Field–Aligned Currents (FACs) even during IMF = 0. They further hypothesized that the quasi-viscous interaction of the solar wind with the magnetosphere lobes may cause sunward convection through the bunch's core, effectively mapping the FACs of northward B_z type down to sub-auroral latitude near the pole area. In an earlier study, Iijima and Potemra[31] found that the FAC direction is persistent in the dawn and dusk sectors of the auroral oval forming the region 1 and region 2 system of the current pattern, where currents near noon at polar cusp latitudes are found to strongly depend on the IMF conditions.

Since Fig. 6 compared the polar and subauroral latitude during quiet time and one can make out the difference in the same external solar wind-IMF forcing. The periodic variations are more pronounced in Maitri than Vostok during quiet time, as we later discuss in Fig. 9 and Fig. 10. Vostok being at polar latitudes more random adulation exists since open magnetic flux is higher than Maitri. It points out that the currents are periodic during magnetic quiet time and cause dawn-dusk convective electric fields in the brim of auroral latitude with semi-diurnal fluctuations as shown at Maitri. When considering the seasonal variability, Fig. 7 and Fig. 8 depict the seasonal dependence of the southern hemisphere. We have used a commonly adopted division viz., April-June, southern winter, and October–December, southern summer. Other months are left due to variability in sunshine hours. The average magnetic potential

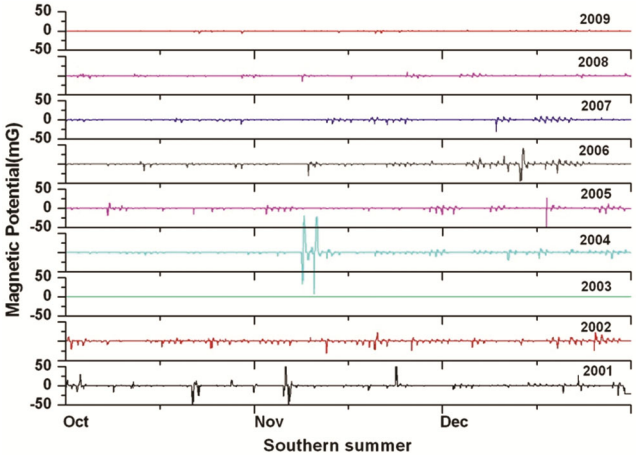

Fig. 7 — Magnetic potential from 2001-2009 years during southern summer months.

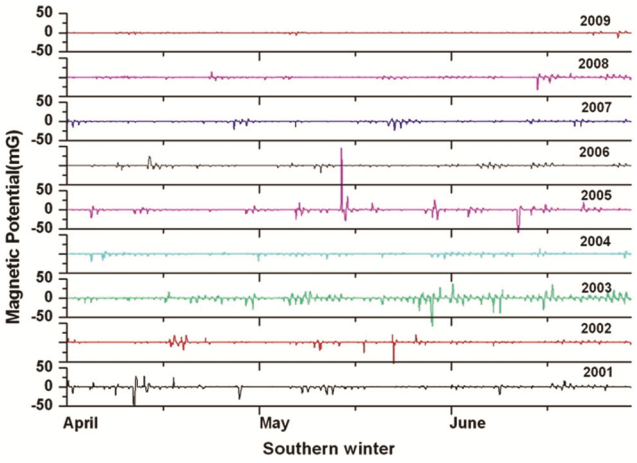

Fig. 8 — Magnetic potential from 2001-2009 years during winter months.

significantly increased in the southern hemisphere during summer. It is natural since solar UV ionization increases Pedersen's conductivity. Spherical cap harmonic analysis for the southern polar region during summer, and winter provided a realistic pattern, parametrized by the IMF component directions and magnitudes.

Earth's orbits may also enhance the asymmetry of magnetic potential distributions because the planet is in its perihelion at the beginning of January and hence the region is lighted and ionized better. Therefore the ionospheric ionization should be slightly larger during this period. The perihelia–aphelion difference in the Sun-Earth distance is about 3% hence the corresponding ionospheric electrodynamics seems to differ due to the close proximity. The major periodicities in external IMF disturbances were identified between 2001-2009 and its magnetic energy modulations and characteristics are shown in Fig. 7 and Fig. 8. Solar events are responsible for positive peaks during (2001- 2003). It diminished drastically during the (2007-2008) solar minimum.

Figure 9, depicts the annual variability of external magnetic potential from 2001 to 2009 years, at Vostok and Fig. 10, for Maitri, Antarctica. Magnetic potential(Ø) saturations often take place Vostok region. It seems to be essentially the result of region 1 currents. Which in turn proves the Hill-Siscore (H-S) hypothesis Hill[32]. In the saturated regime according to the H-S formulation, $\Phi = 57.6\ {}_{(r)}P^{(2/3)}/p^{(1/2)}+0.012\zeta p$, ${}_rP$ is the solar wind ram pressure, ζ - a factor that depends on the geometry of currents flowing into the ionosphere, p the ionospheric Pedersen conductance.

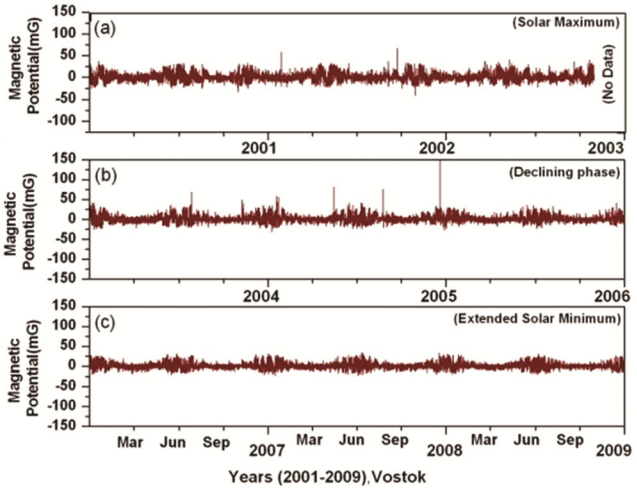

Fig. 9 — External magnetic potential from 2001-2009 years, Vostok, Antarctica.

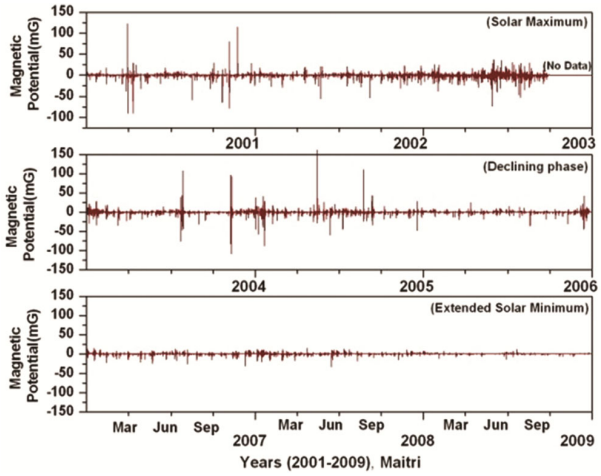

Fig. 10 — External magnetic potential from 2001-2009 years, Maitri, Antarctica.

In the saturated regime according to the H-S formulation, the magnetosphere acts as a constant current generator with a magnitude determined by the strength of the region 1 current system. $\sum_P$ In this scenario, the ionospheric Ohm's law can be written as $I_1 = \xi \sum P\Phi_{pc}$ and Φ_{pc} depends inversely on $\sum_P$ Since Region 1 current reconfigures up and eventually replace the Chapman-Ferraro currents at the magnetopause and provide the *J x B* force to hold solar wind ram pressure[33]. The limitation of the ram pressure to hold off the solar wind defines the size of the region 1 currents and hence ∇x H saturate at the polar region.

The quantitative external response of the geomagnetic potential is a function of solar wind velocity (V_{sw}), number density (N_{sw}) of the solar wind (SW), and interplanetary magnetic field (IMF) - B_y and B_z and clock angle (φ),[14]. Ranges of satellite data on various aforesaid parameters enable one to know behavior of magnetic potential of the high latitudes. For Vostok and Maitri we further did correlation and regression analysis (figures are not shown) and we got the regression equation as $\Delta\theta\ (\mathrm{nT}) = 26.17 + 4.5 N_{sw} V_{SW} B_T sin^4(\theta/2)$. This equation is more suitable for Vostok station than for Maitri. Fig. 10 indicates results of Maitri in the subauroral latitudes, the magnetic potential is complex. It may be due to the fact that induced field lines are connected with closed magnetosphere during sub-storms and the intense electric fields are produced only during geomagnetic perturbations which drive a system of currents. During this situation, peaks or enhancement in external magnetic potential can be observed in Maitri only during aforesaid disturbances. At this juncture, it is important in the sense that for analyzing non-linear dynamical characteristics of the system and their interplay regarding solar wind forcing statistical correlation functions alone may not be adequate.

4 Conclusions

The scientific research is the first of its kind by employing spherical cap harmonic analysis measures for studying the variations of dynamical characteristics of solar wind coupling to the high latitude magnetosphere-ionosphere system. The study is important in the sense that for analyzing non-linear dynamical characteristics of magnetosphere-ionosphere systems and their interplay regarding solar wind forcing. This research study analyzes different periodicities associated with solar activity and its associated magnetic potential energy modulations observed over southern high latitudes. The external response of the magnetic potential is a multiplication scale factor for each individual characteristic component of IMF and solar wind parameters. The inference indicates that the magnetic potential at Maitri depends on the magnitudes of the induced field lines which are extended to subauroral latitudes. During this scenario in Maitri there are noticeable peaks or enhancements in magnetic potential which can be observed mainly during geomagnetic disturbances.

Acknowledgment

The authors are grateful to the Director, Indian Institute of Geomagnetism, Navi Mumbai for constant support and the Ministry of Science and Technology, Government of India, for financial assistance. We also thank Dr. D R Weimer for providing his IDL-based SCHA- the model for computing the magnetic potential. The authors acknowledge the ACE satellite team for the solar wind and IMF data.

References

1 Chapman S & Bartels J J, *Geomagnetism*, 25 (1940) 62.
2 Chapman S & Ferraro V C A, *Terr Magn Atmos Electr*, 36 (1931) 77.
3 Besse J & Courtllot V, *J Geophys Res*, 107, (2002) B11.
4 Newell P T, Sotirelis T, Liou K, Meng C I & Rich F J, *J Geophysics Res*, 112 (2007) 1.
5 Knipp D J, *J Geophys Res*, 103 (1998) 26197.
6 Lu G, *et al*., *J Geophys Res*, 103 (1998) 11685.
7 Stamper R, Lockwood M, Wild M N & Clark T, *J Geophys Res*, 104 (1999) 28325.
8 Kallio E I, PulkkinenT I, ,Koskinen H E J, Viljanen A & Slavin J A, *Geophys Res Lett*, 27 (2000) 1627.
9 Akasofu S I, *Space Sci Rev*, 28 (1981)121.

10 Tanskanen E I, Pulkkinen T I & Koskinen H E, *J Geophys Res*, 107 (2002) 1086.
11 Anil Kumar C P & Venugopal C, *Ind J Phys*, 77 (2003) 277.
12 Lowrie W, *Geophysical Equations*, Cambridge University Press, 2011.
13 Lowes F J, *J Geophys Res*, 71 (1966) 2179.
14 Weimer D R, *J Geophys Res*, 110 (2005) A12307.
15 Campbell W H & Schiffmacher E R, *J Geophys Res*, 90 (1985) 6745.
16 Campbell W H & Schiffmacher E R, *J Geophys Res*, 93 (1988) 933.
17 Alldredge L, *J Geophys Res*, 86 (1981) 3021.
18 Haines G V, *J Geophys Res*, 90 (1985) 2583.
19 Korte M & Holme R, *Geophys J Int*, 153 (2003) 253.
20 Sutcliff P R, *Ann Geophysicae*, 18 (1999) 120.
21 Gonzalez W D & Gonzalez A, *Planet Space Sci*, 32 (1984) 1007.
22 Turner N E, Cramer W D, Earles S K & Emery B A, *J Atmos Sol-Terr Phys*, 71 (2009) 1023.
23 Knipp D J, *J Geophys Res*, 103 (1998) 26197.
24 Tanskanen E I, PulkkinenT I & Koskinen H E J, *J Geophys Res*, 107 (2002) 1086.
25 Iyemori T, Takeda M, Odagi Y & Toh H, Mid-latitude geomagnetic indices ASY-H and SYM-H for 2009, International report WDC: 2010; KyotoUniversity, Japan.
26 Campbell W H, *J Geophys Res*, 84 (1979) 875.
27 Gonzalez W D, Joselyn J A, Kamide Y, Kroehi H W, Roster G, Tsurutani B T & Vasyliunus V M, *J Geophys Res*, 99 (1994) 5771.
28 Wang Y M, Ye P Z, Wang S , Zhou G P & Wang J X, *J Geophys Res*, 107, A11 (2002) 1340.
29 Somayajulu V V, *Proc Ind Sci Acad*, 64 (1998) 341.
30 Papitashvili V O , Christiansen F & Neubert T, *Geophys Res Lett*, 28 (2001) 3055.
31 Iijima T & Potemra T A, *J Geophys Res*, 81 (1976) 5971.
32 Hill T W, Dessler A & Wolf R A, *Geophys Res Lett*, 3 (1976) 429.
33 Siscoe G L, Etricson T M, Sonnerup B U O , Maynard N C, Schoendorf J A, Siebert K D, Weimer D R, White W W & Wilson G R, *J Geophys Res*, 107 (2002) 1075.